22. For correlation analyses of subsets of object-selective cortex, the category that elicited the maximal response in each voxel was determined for even runs, odd runs, and all runs. To examine whether the pattern of response to a category could be discerned in cortex that responded maximally to other categories, we restricted comparisons of responses to pairs of categories to voxels that did not respond maximally to either category on either even or odd runs. This was the most exacting test of this prediction that we could devise. To examine the response in regions that responded maximally to only a single category (faces, houses, or cats) or to only small man-made objects, we included only those voxels that had maximal responses averaged across all runs. Thus, there was no overlap between these regions.
23. The image data were not smoothed before analysis; nonetheless, it is possible that voxels outside of the regions showing maximal responses to a given category could still be influenced by the maximally responsive region because of spatial smoothness due to imaging techniques and partial volume effects. To address this issue, we also analyzed our data after excluding all voxels that responded maximally to the two categories being compared as well as all voxels that were adjacent to these regions. On average, this analysis excluded 58% of voxels from the calculation of correlations. Nonetheless, overall accuracy for identifying the category being viewed was 92%, demonstrating that the results are not attributable to the effect of maximally responsive regions on adjacent voxels.
24. Supplemental data are available on *Science* Online at www.sciencemag.org/cgi/content/full/293/5539/2425/DC1.
25. Within the region that responds maximally to faces, sites may exist that respond exclusively to faces that are interdigitated with sites that respond maximally, but not exclusively, to faces, as suggested by studies of evoked potentials recorded with electrodes on the cortical surface (*44*). It is important to note, however, that most face-selective recording sites in these studies do show some response to other objects and even the sites that demonstrate an N200 response exclusively to faces appear to respond to other objects also but with different latencies.
26. E. Hering, *Outlines of a Theory of the Light Sense* (Harvard Univ. Press, Cambridge, MA, 1964).
27. L. M. Hurvich, D. Jameson, *Psychol. Rev.* **64**, 384 (1957).
28. R. L. De Valois, *Cold Spring Harbor Symp. Quant. Biol.* **30**, 567 (1965).
29. I. Biederman, *Psychol. Bull.* **94**, 115 (1987).
30. A. J. O'Toole, H. Abdi, K. A. Deffenbacher, D. Valentin, *J. Opt. Soc. Am. A* **10**, 405 (1993).
31. P. J. B. Hancock, A. M. Burton, V. Bruce, *Mem. Cognit.* **24**, 26 (1996).
32. A. Lanitis, C. J. Taylor, T. F. Cootes, *IEEE Trans. Pattern Anal. Mach. Int.* **19**, 743 (1997).
33. V. Blanz, A. J. O'Toole, T. Vetter, H. A. Wild, *Perception* **29**, 885 (2000).
34. D. A. Leopold, A. J. O'Toole, T. Vetter, V. Blanz, *Nature Neurosci.* **4**, 89 (2001).
35. H. Hecaen, R. Angelergues, *Arch. Neurol.* **7**, 24 (1962).
36. A. Damasio *et al.*, *Neurology* **32**, 331 (1982).
37. E. K. Warrington, T. Shallice, *Brain* **107**, 829 (1984).
38. Of the category-selective agnosias, only prosopagnosia is a purely visual agnosia, and controversy still exists over whether a pure prosopagnosia exists that has no effect on other aspects of visual object perception (*45*). Other category-selective agnosias also involve loss of nonvisual knowledge about the affected category and are associated with lesions in cortices other than those of the ventral temporal lobe (*37*). The literature on lesions that cause prosopagnosia is uninformative about what part of ventral temporal cortex is critical for face recognition. The lesions that cause prosopagnosia tend to be large (*37*). It has never been demonstrated that the critical part of lesions that cause prosopagnosia involves damage to the small region that responds maximally to faces. For a lesion to cause prosopagnosia, it may require damage in regions that show the most modulation of response to different individual faces, which may not be coextensive with the region that responds maximally to faces, or damaged connections to cortices in other parts of the brain that are critical for face recognition, such as the superior temporal sulcus or the anterior temporal cortex.
39. Models of the functional architecture of ventral extrastriate cortex that focus analysis on mean responses in regions that are putatively specialized for stimulus category (*5, 7*) or perceptual process (*9–11*) are not inconsistent with a coexisting functional architecture that embodies the distinct representations for all categories. Unlike the object form topography model proposed here, however, these specialized region models do not provide an explicit account for how such a coexisting functional architecture is organized or how the representations for an unlimited variety of categories could differ from each other within this architecture.
40. J. V. Haxby, J. M. Maisog, S. M. Courtney, in *Mapping and Modeling the Human Brain*, P. Fox, J. Lancaster, K. Friston, Eds. (Wiley, New York, in press).
41. J. Talairach, P. Tournoux, *Co-Planar Stereotoxic Atlas of the Human Brain* (Thieme, New York, 1988).
42. J. V. Haxby, E. A. Hoffman, M. I. Gobbini, *Trends Cognit. Sci.* **4**, 223 (2000).
43. A. Martin, L. G. Ungerleider, J. V. Haxby, in *The New Cognitive Neurosciences*, M. S. Gazzaniga, Ed. (MIT Press, Cambridge, MA, 1999), pp. 1023–1036.
44. T. Allison, A. Puce, D. D. Spencer, G. McCarthy, *Cereb. Cortex* **9**, 415 (1999).
45. I. Gauthier *et al.*, *J. Cogn. Neurosci.* **12**, 495 (2000).

46. We would like to thank R. Desimone, A. Martin, L. Pessoa, G. Ronca, and L. Ungerleider for discussion and comments on earlier versions of this paper.

22 June 2001; accepted 6 August 2001

REPORTS

Field-Induced Superconductivity in a Spin-Ladder Cuprate

J. H. Schön,[1,2*] M. Dorget,[3,4] F. C. Beuran,[4] X. Z. Xu,[4] E. Arushanov,[4,5] M. Laguës,[4] C. Deville Cavellin[3,4]

We report on the modulation of the transport properties of thin films, grown by molecular beam epitaxy, of the spin-ladder compound $[CaCu_2O_3]_4$, using the field effect in a gated structure. At high hole-doping levels, superconductivity is induced in the nominally insulating ladder material without the use of high-pressure or chemical substitution. The observation of superconductivity is in agreement with the theoretical prediction that holes doped into spin ladders could pair and possibly superconduct.

Because of the prediction of the presence of spin-gap and possible appearance of d-wave superconductivity, much attention has been paid to the so-called spin-ladder systems (*1–4*). Ladder systems are considerably easier to study theoretically than two-dimensional models, because they are basically quasi–one-dimensional and they can provide a playground for studies of high–critical temperature (high-T_c) superconductors (*4*). Spin-ladder systems, especially two-leg ladders (Fig. 1), are interesting model materials to investigate low-dimensional quantum systems. Two-leg ladders are essentially one-dimensional (1D), and doped ladders are a fascinating mixture of a dilute Fermi gas with strong attractions and a concentrated Fermi system with a large Fermi surface (*3*). In addition, the similarities between doped ladders and doped CuO_2 planes make for interesting comparison. However, a difficulty that arises in the preparation of undoped and doped materials is that structural changes due to chemical doping may mask the effect of the change of the doping level and that doping-induced disorder might suppress the observation of superconductivity. It has been shown that the modulation of the carrier concentration leading, for example, to gate-induced superconductivity is a powerful tool to study the electronic properties of various materials as a function of the doping level (*5–9*), which circumvents the issue of doping-induced disorder.

So far, only Sr-rich $Sr_{1-x}Ca_xCu_2O_3$ and $(Sr_{1-x}Ca_x)_{14}Cu_{24}O_{41}$ materials, prepared under

[1]Bell Laboratories, Lucent Technologies, 600 Mountain Avenue, Murray Hill, NJ 07974–0636, USA. [2]University of Konstanz, Department of Physics, Post Office Box X916, D-78457 Konstanz, Germany. [3]Groupe de Physique des Milieux Denses, Université Paris XII, 61 Avenue du Général de Gaulle, 94010 Créteil Cedex, France. [4]Surfaces et Supraconducteurs CNRS UPR5-ESPCI, 10 Rue Vauquelin, 75005 Paris, France. [5]Institute of Applied Physics, Academy of Sciences of the Moldova Republic, Academiei str. 5, Kishinev 277028, Moldova.

*To whom correspondence should be addressed. E-mail: j.hendrix@ratskrone.de

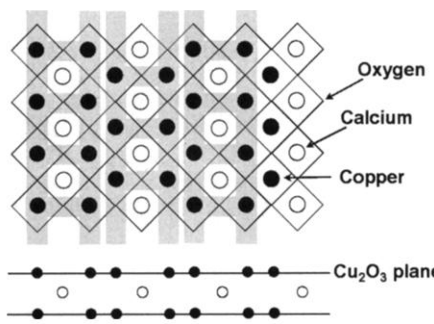

Fig. 1. Schematic structure of the two-leg ladder compound $[CaCu_2O_3]_4$.

high pressure (*10*) or by the float-zone technique (*11, 12*), were studied because of the difficulties of preparing pure Ca compounds (x = 1). Recently, high-quality $[CaCu_2O_3]_4$ (*13*) and $Ca_{14}Cu_{24}O_{41}$ (*14*) thin films as well as bulk $Ca_{14}Cu_{24}O_{41}$ (*15*) and $CaCu_2O_3$ single crystals (*16*) were prepared and characterized. In an undoped two-leg spin-ladder, the existence of the spin-gap in the magnetic excitation spectrum was confirmed for $SrCu_2O_3$ (*17*) and $Sr_{0.4}Ca_{13.6}Cu_{24}O_{41}$ (*18–20*). Stimulated by theoretical work, numerous experiments have been performed in order to search for superconducting properties in even-leg materials. In the doped $Sr_{0.4}Ca_{13.6}Cu_{24}O_{41}$, $Sr_2Ca_{12}Cu_{24}O_{41}$, and $Ca_{14}Cu_{24}O_{41}$, superconductivity was observed under high pressure (≥3 GPa) with a maximum at 12 to 13 (*19, 20*), 5 (*21*), and 8 K (*15*), respectively. The structure of $(Sr_{1-x}Ca_x)_{14}Cu_{24}O_{41}$ consists of two distinct Cu-O sublattices: Cu_2O_3 (two-leg ladder) planes with CuO_2 chains (1D chains of CuO_4 squares with shared edges) alternately stacked along the *c*-axis of the orthorhombic cell (*10*). It is assumed that the main effect of high pressure in the aforementioned compounds is the hole redistribution between CuO_2 chains and the Cu_2O_3 ladder sheets. Under high pressure, the hole density

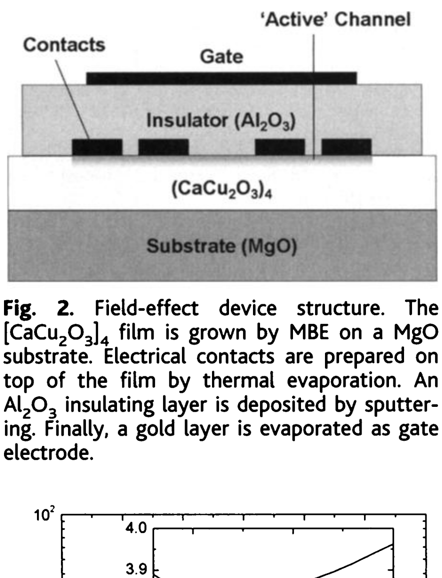

Fig. 2. Field-effect device structure. The $[CaCu_2O_3]_4$ film is grown by MBE on a MgO substrate. Electrical contacts are prepared on top of the film by thermal evaporation. An Al_2O_3 insulating layer is deposited by sputtering. Finally, a gold layer is evaporated as gate electrode.

in the ladders is expected to increase (*20*), which should be the origin of the observed superconducting properties. However, it remains to be investigated whether this phase corresponds to the theoretically predicted superconductivity on the basis of the analysis of isolated ladder (*4*). It is also worth mentioning that transport and copper-63 nuclear magnetic resonance measurements of the Knight shift and relaxation time T_1 performed on $Sr_2Ca_{12}Cu_{24}O_{41}$ single crystals as a function of pressure show a collapse of the gap in spin exitations when superconductivity is stabilized at 3.1 GPa (*21*).

For bulk Cu_2O_3 pure ladder systems, the attempts to dope the compounds were not successful, and superconductivity as theoretically predicted was not yet observed. On the other hand, it is possible to dope molecular beam epitaxy (MBE)–grown $[CaCu_2O_3]_4$ films (*22*) in the range of 0.12 to 0.25 electron per copper atom. Here, we report on the observation of superconductivity in a $[CaCu_2O_3]_4$ ladder thin film induced by the field-effect at ambient pressure. The maximum transition temperature T_c is, at 14 K, slightly above the value reported for chemically doped bulk samples under pressure (*19, 20*).

The film, 30 nm thick, was grown by MBE on a MgO (100) substrate (*13*). The crystal structure and composition were determined, using four-circle x-ray diffraction, high-resolution transmission electron microscopy, and Rutherford backscattering. A new type of stacking of the ladder planes was observed in these compounds. The ladders stack by dimers, formed by two perfectly superposed ladder planes, separated by a Ca plane. Between two neighboring dimers, there is a shift in the direction of the ladder legs. The crystal cell thus contains four ladder planes, with 0.31 nm separating two consecutive ladder planes. It is interesting to note that this $[CaCu_2O_3]_4$ compound is at least 10% more compact than the corresponding $CaCu_2O_3$ bulk compound with no shift between dimers. This is in agreement with the higher level of oxidation in the films, possibly due to a new type of oxygen site related to the shift between dimers. This site is absent in the bulk $CaCu_2O_3$ compounds. Because of the lattice mismatch, some residual strain will be present in the MBE-grown films.

Field-effect devices were prepared on top of the MBE-grown 30-nm-thick $[CaCu_2O_3]_4$ films (Fig. 2). As a first step, gold pads were thermally evaporated for electrical measurements mainly along the ladder legs. However, twinning in the sample prohibited a perfect orientation of the sample. Secondly, a gate insulator, Al_2O_3, was deposited by radio frequency–magnetron sputtering (*5–9*). The capacitance of this layer is 120 nF/cm^2. Finally, a gold gate electrode is deposited on top of the insulating layer. By applying a negative voltage to the gate, the doping level in the active channel at the insulator/$[CaCu_2O_3]_4$ film interface can be modulated. It is worth mentioning that this hole accumulation layer extends only a few nanometers (around one ladder plane) into the thin film. Hence, only a thin interface layer becomes superconducting at very high gate bias.

The as-grown thin film exhibits metallic behavior above ~220 K, whereas the charge transport is governed by variable-range hopping below 150 K (Fig. 3) (*23*). The metallic behavior at high temperatures shows that even the as-grown layers are heavily doped. By applying a negative voltage to the gate, a distinct transition from insulating (below 150 K) to metallic transport is observed (Fig. 4). Moreover, for a gate charge of approximately 9×10^{13} cm^{-2}, the resistance of the film drops to zero, indicating a transition to a superconducting phase. Assuming a homogeneous hole distribution in the ladder plane, the onset of the superconductivity corresponds to a doping level of approximately 0.1 hole per Cu atom, which is significantly less than in bulk samples under pressure (*24*). Interestingly, the two-dimensional superconductor-insulator transition takes place close to the universal value of $h/(4e^2)$. Similar behavior has been observed in bulk-doped samples

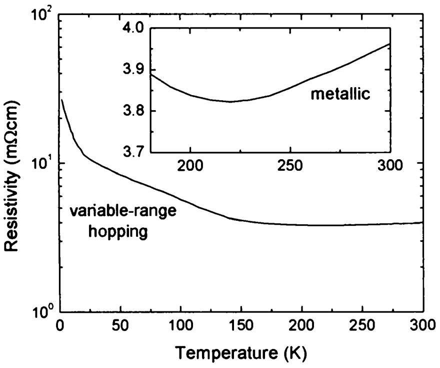

Fig. 3. Resistivity per ladder plane of an as-grown $[CaCu_2O_3]_4$ film as a function of temperature. Below 150 K, the transport is governed by variable range hopping. Above ~220 K, metallic behavior is observed (see inset).

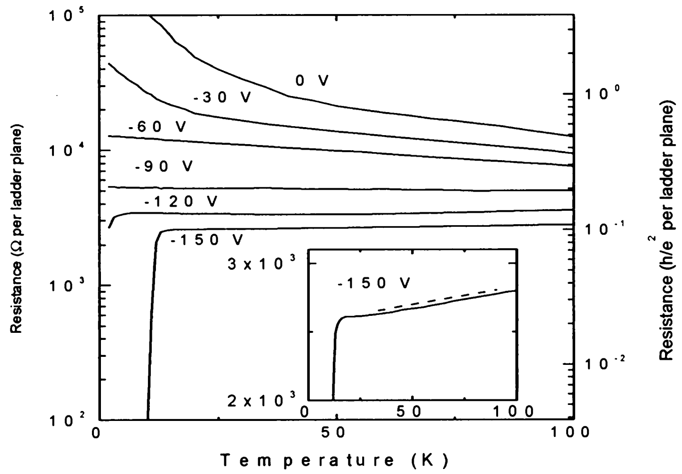

Fig. 4. Resistance per ladder plane of a $[CaCu_2O_3]_4$ film as a function of temperature and the applied gate bias. A transition from insulating to metallic and, finally, to superconducting behavior is observed. The inset shows the resistance at −150 V on a linear scale. The dashed line corresponds to a linear dependence.

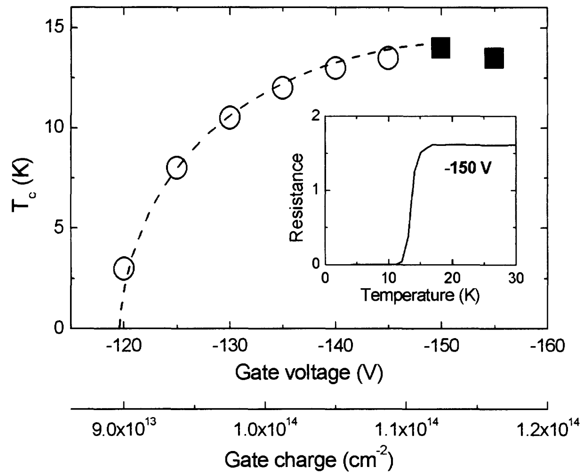

Fig. 5. Superconducting transition temperature T_c as a function of gate bias. A maximum T_c of 14 K is achieved for a gate bias of −150 V. The gate charge is calculated from the capacitance of the insulating layer and the applied voltage. The inset shows the superconducting transition. The open and solid symbols indicate insulating ($d\rho/dT < 0$) and metallic ($d\rho/dT > 0$) behavior, respectively, above T_c.

(*25*). The transition temperature T_c increases gradually up to a maximum value of 14 K for the highest gate voltages possible (Fig. 5), which is slightly higher than for ladder materials at high pressure (*19*, *20*). The experimental range is limited by the breakdown strength of the Al_2O_3 layer. The residual resistivity per ladder plane is slightly less than for bulk single-crystal samples (*25*), revealing the high quality of the MBE-grown films. In the inset of Fig. 4, a linear dependence of the resistivity ρ above T_c can be observed, which is similar to doped two-dimensional cuprates (*26*). Moreover, note that the temperature dependence above T_c changes from insulating ($d\rho/dT < 0$) to metallic ($d\rho/dT > 0$) around optimal doping (maximum T_c) (Fig. 5). In addition, the superconducting transition shifts to lower temperatures by the application of a magnetic field perpendicular to the field-effect structure. A superconducting coherence length parallel to the ladder direction of 40 Å can be estimated from the suppression of the superconductivity (*27*). The observation of superconductivity in this two-leg ladder compound is in accordance with the theoretical prediction that hole doping of such materials should lead to pairing and superconductivity.

Our results demonstrate that field-effect doping is a very powerful technique to study electrical properties as a function of doping-level without inducing structural changes or additional disorder. The study of metal-insulator transitions or superconductivity in $[CaCu_2O_3]_4$ are only some possibilities. We envision that this method can be extended to other ladder compounds as well as other materials in order to search for superconductivity as well as to test theoretical predictions.

References and Notes

1. E. Dagotto, J. Riera, D. Scalapino, *Phys. Rev. B* **45**, 5744 (1992).
2. T. M. Rice, S. Gopalan, M. Sigrist, *Europhys. Lett.* **23**, 445 (1993).
3. E. Dagotto, T. M. Rice, *Science* **271**, 618 (1996).
4. E. Dagotto, *Rep. Prog. Phys.* **62**, 1525 (1999).
5. J. H. Schön, Ch. Kloc, R. C. Haddon, B. Batlogg, *Science* **288**, 656 (2000).
6. J. H. Schön, Ch. Kloc, B Batlogg, *Nature* **406**, 704 (2000).
7. ———, *Nature* **408**, 549 (2000).
8. J. H. Schön *et al.*, *Nature* **410**, 189 (2001).
9. C. H. Ahn *et al.*, *Science* **284**, 1152 (1999).
10. E. M. McCarron, M. A. Subramanian, J. C. Calabrese, R. L. Harlow, *Mater. Res. Bull.* **23**, 1355 (1988).
11. A. Revcolevschi, J. Jegoudez, *Coherence in High Temperature Superconductors*, G. Deutscher, A. Revcolevschi, Eds. (World Scientific, Singapore, 1996).
12. A. Revcolevschi, A. Vietkine, H. Mouden, *Physica C* **282–287**, 493 (1997).
13. C. Deville Cavellin *et al.*, *Physica C* **282-287**, 929 (1997).
14. Y. Furubayashi *et al.*, *Phys. Rev. B* **60**, R3720 (1999).
15. S. M. Kazakov, J. Karpinski, G. I. Meijer, C. Bougerol-Chaillout, M. Nunez-Regueiro, *Physica C* **351**, 301 (2001).
16. V. Kiryukhin *et al.*, *Phys. Rev. B* **63**, 144418 (2001).
17. M. Azuma, Z. Hiroi, M. Takano, Y. Ishida, Y. Kitaoka, *Phys. Rev. Lett.* **73**, 3463 (1994).
18. R. S. Ecclestona, M. Azuma, M. Takano, *Phys. Rev. B* **53**, R14721 (1996).
19. M. Uehara *et al.*, *J. Phys. Soc. Jpn.* **65**, 2764 (1996).
20. M. Isobe *et al.*, *Phys. Rev. B* **57**, 613 (1998).
21. H. Mayaffre *et al.*, *Science* **279**, 345 (1998).
22. M. Dorget *et al.*, *Physica C* **341-348**, 477 (2000).
23. C. Partiot *et al.*, *Physica C* **341-348**, 475 (2000).
24. T. Osafune, N. Motoyama, H. Eisaki, S. Uchida, *Phys. Rev. Lett.* **78**, 1980 (1997).
25. T. Nagata *et al.*, *Phys. Rev. Lett.* **81**, 1090 (1998).
26. M. B. Maple, *J. Magn. Magn. Mater.* **177-181**, 18 (1998).
27. The anisotropy of the coherence length within the ladder plane was not taken into account explicitly; it will be an interesting topic for further studies [see, for example, T. Nakanishi *et al.*, *Physica B* **281-282**, 975 (2000)].

28. We are grateful to Ch. Kloc and C. M. Varma for valuable discussions. One of us (F.C.B.) would like to thank the company WINTICI for financial support.

9 July 2001; accepted 22 August 2001

High-Temperature Superconductivity in Lattice-Expanded C_{60}

J. H. Schön,[1,2]* Ch. Kloc,[1] B. Batlogg[1,3]

C_{60} single crystals have been intercalated with $CHCl_3$ and $CHBr_3$ in order to expand the lattice. High densities of electrons and holes have been induced by gate doping in a field-effect transistor geometry. At low temperatures, the material turns superconducting with a maximum transition temperature of 117 K in hole-doped $C_{60}/CHBr_3$. The increasing spacing between the C_{60} molecules follows the general trend of alkali metal–doped C_{60} and suggests routes to even higher transition temperatures.

The superconducting properties of various materials can be modulated by the application of an electric field, and a variety of field-effect devices have been studied lately (*1*–*9*). We recently demonstrated the switching between insulating and superconducting behavior in single crystals of C_{60}. The gate-induced superconductivity is observed for electron doping (*5*) as well as hole doping (*7*). The higher superconducting transition temperature (T_c) for hole doping may be ascribed to a larger density of states at the Fermi level and stronger coupling to phonons (*8*, *10*, *11*). C_{60} is a particularly interesting superconductor because the dominant electron-phonon interaction, being an on-site intramolecular property, can be conceptually separated from the electronic density of states, which is given by the distance between adjacent molecules. Expanding the lattice, therefore, increases the density of states, and the resulting increase of T_c is well documented in alkali metal–doped bulk samples (A_3C_{60}) (*12*, *13*). The observation of gate-induced hole doping of C_{60} resulting in a T_c of 52 K suggests that significantly higher T_c's could be anticipated in suitably "expanded" C_{60} crystals. Indeed, here we report on raising T_c to 117 K with such methods.

Undoped C_{60} single crystals have been grown from the vapor phase in a stream of hydrogen (*14*). $CHCl_3$ and $CHBr_3$ are interca-

[1]Bell Laboratories, Lucent Technologies, 600 Mountain Avenue, Murray Hill, NJ 07974, USA. [2]University of Konstanz, Department of Physics, D-78457 Konstanz, Germany. [3]Solid State Physics Laboratory, Eidgenössische Technische Hochschule, CH-8093 Zürich, Switzerland

*To whom correspondence should be addressed. E-mail: hendrik@lucent.com